SHRINKABLE SILICONE THIN MEMBRANES AND THEIR INTEGRATION IN 3D PRINTED MICROFLUIDIC OXYGENATORS

Anand Sojan[1], Ponnambalam Ravi Selvaganapathy[1], and Islam Hassan[1]*
[1]Department of Mechanical Engineering, McMaster University, Ontario, Canada

ABSTRACT

This work introduces a hybrid additive manufacturing technique, to overcome the constraints associated with the current lithography-based device fabrication of microfluidic blood oxygenators. The described approach sequentially combines: (i) sacrificial templating of isomalt to form embedded microchannels and (ii) controlled shrinking of silicone to form thin gas exchange membranes sandwiching the channels. This eliminates the need for cleanroom-based manufacturing, membrane bonding and potential device assembly. Devices based on polydimethylsiloxane (PDMS) membranes with thickness <100µm and microchannels with dimensions <150µm was achieved. This method offers a promising next step for manufacturing scalable microfluidic oxygenators and integrated non-planar lung assist devices.

KEYWORDS

Microfluidic devices, Oxygenators, 3D printing, Sacrificial scaffolding, Silicone shrinking

INTRODUCTION

Current Extracorporeal Membrane Oxygenation (ECMO) comprising of hollow-fiber membrane oxygenators (HFMOs) is limited by the intricacy of the blood circuit and risk to blood health. The advancements in microfluidic device design and production technology have led to the emergence of microfluidic-based oxygenators that can be adjusted to specific requirements. These scaled-down artificial lungs provide benefits such as reduced initial blood volume and minimized contact area. By manipulating the size and structure of the vascular channel networks, they replicate the natural path of blood flow. In this type of system, blood is channeled through intricate microfluidic pathways, with oxygenation occurring through a gas-permeable membrane via the diffusion of oxygen from the gas side to the blood side [1]. Microfluidic Blood Oxygenators (MBOs) serve as a potential alternative to HFMOs, with various groups having demonstrated promising oxygen transfer efficiencies for both in-vitro MBOs [2–4] and in-vivo studies [5–7]. MBOs are mostly manufactured by using a master mold fabricated by conventional lithography [8]. This gives well-defined microchannels for blood oxygenators. However, the scalability of this approach is limited by the fabrication constraints associated with these 2D patterning techniques. The current approach relies on successfully bonding the thin patterned layer with the thin gas exchange layer [5]. This bonding of an uncured PDMS layer with the patterned cure-layer can provide a high bonding strength, up to about 671 kPa [9]. However, successfully bonding such thin large area membrane top layer with the uncured base requires careful handling. The probability of entrapping air bubbles, uneven leakage of uncured PDMS into the microchannels and failure in localized bonding pose further operational challenges. These factors affect the yield of device production and require multi-step clean room processes for their fabrication which requires significant time and resource commitments. Photolithographically patterning the master mold is constrained by the maximum wafer size that can be exposed and its availability, which is usually limited to either 8 or 12inch wafers, necessitating the incorporation of denser networks in a single unit. Hence, to enhance the capacity for gas exchange, it is necessary to produce devices with larger surfaces for gas exchange and stack multiple layers to meet oxygenation demands. The resulting manufacturing involves the stacking of parallel layers, which requires interconnections that consume a significant portion of the blood volume and increases the device form factor.

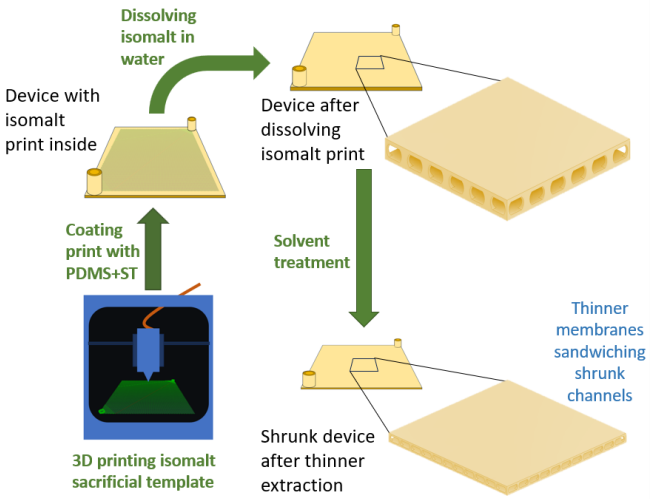

Figure 1: Hybrid manufacturing of embedded microchannels in thin membranes by sequential sacrificial templating and shrinking of silicone

Additive manufacturing (AM)-based fused deposition of sacrificial materials is an avenue currently explored in microfluidics [10]. Although scalable, resolutions achievable with these approaches are not comparable to lithography-based manufacturing and hence there is a need to further develop this approach. Our hybrid manufacturing technique employs isomalt as sacrificial material to form water-soluble scaffolds inside a membranous silicone matrix, which shrinks upon solvent treatment. Isomalt is a sugar substitute that easily dissolves in water and the printed isomalt leaves behind hollow embedded channels [10,11] upon dissolution. The gas exchange membrane is made from a polydimethylsiloxane (PDMS) based formulation with definite weight ratio of silicone thinner (ST). When the cured PDMS-thinner construct is treated in a suitable solvent bath, it initiates the swelling of the PDMS and the thinner leaches out. Once dried, this leads to shrinkage in dimensions, leading to smaller channels and thinner membranes.

PRINCIPLE

Sacrificial templating for microchannel formation

The majority of carbohydrate glass blends can be prepared by melting them at temperatures exceeding 90 °C to reduce viscosity, allowing smooth extrusion through the nozzle during the printing process. When cooled below its glass transition temperature, they solidify into a desired shape, making it advantageous for 3D printing purposes [11]. Unlike other sugars that undergo crystallization when kept above their glass transition temperature for prolonged time, isomalt crystallizes by forming dihydrates, which can be prevented or slowed down by dehydration. Characterization study of isomalt using cyclic DSC indicated that once the thermal history was

978-1-940470-05-4/HH2024/$25©2024TRF
DOI 10.31438/TRF.HH2024.68

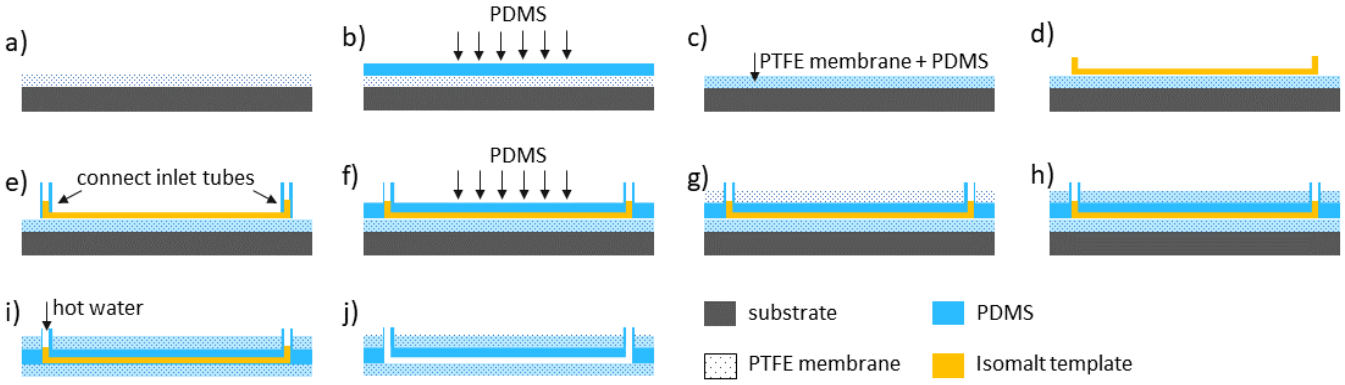

Figure 2: Step-by-step process flow of proposed device fabrication technique

eliminated, isomalt glass exhibited a uniform thermal profile during a cyclic heating-cooling process [12]. Adhering to this procedure for erasing the thermal history can maintain isomalt in a stable glassy state throughout the printing process. Furthermore, the subsequent release of isomalt from the channels does not need any chemicals and can be achieved by using a hot water bath.

Shrinking of Silicone matrix

The silicone coating/casting is formulated with specific weight ratio of polydimethylsiloxane (PDMS) and silicone thinner (ST). The trapped ST molecules are confined in the cured PDMS matrix and are released by solvent extraction. When the cured PDMS-thinner construct is treated in a suitable solvent bath, it initiates the swelling of the PDMS and the thinner leaches out. Once the thinner is completely extracted in the identified treatment window, the swollen PDMS with trapped solvent is dried in an oven, which vaporizes the solvent, leaving behind the shrunk PDMS matrix.

MATERIALS AND METHODS

3D printing of sacrificial isomalt templates

Custom G-codes were written for all the 3D printing designs and were imported into CAMotics (Cauldron Development LLC) for tool path visualization. The fused filament fabrication (FFF) system consists of an XYZ positioner stage (based on UNI-PRINT-3D printer, "The Cool Tool" GmbH), a metal barrel holding the isomalt assembled with an external heating jacket and enclosed in a metal holder. Metal nozzles (Allevi, 3D Systems) with luer-lock and circular cross-section (Ø400µm) were used. Additionally, the extrusion is realized by an integrated pneumatic control system, synchronized with the XYZ positioner by using the machine interface developed by "The Cool Tool" [13]. Granular isomalt (Lorann, USA) was purchased from a local vendor. Isomalt was filled in the 10cc metal barrel, subjected to heating at 200˚C for 20 minutes and cooled down to room temperature, prior to loading the barrel in the printhead. Combination of printhead-bed temperatures were tested, and the subsequent printing were implemented by maintaining the barrel temperature at 110˚C (exact nozzle temperature unknown) and bed at a temperature of 55˚C (slightly higher than T_g of isomalt). Printed structures were analyzed by using ImageJ, with images taken under EVOS XL microscope (Thermo Fisher Scientific, USA).

Shrinking of silicone thin membranes

To characterize shrinking of silicone, PDMS (monomer and curing agent mixed in 10:1) was mixed with Silicone Thinner (Smooth-On Inc.) and cast into xurographically cut acrylic wells (20mm x 20mm) with thickness <500µm and cured at 90˚C for 30 minutes to form thin membranes. These membranes were solvent treated in excess of solvents to swell the PDMS and extract out the thinner from the matrix. Initial experiments were conducted to identify the time required for complete extraction of thinner (70% wt) by monitoring the weight loss of the sample, until the weight reduced to 30%. To characterize the effect of silicone thinner on shrinking, the concentration of thinner in the mixture was varied from 0% to 80% by weight. Different solvents capable of swelling the PDMS was used in solvent treatment to study the choice of solvent for optimum shrinkage. Post solvent treatment, all samples were dried in ambient room temperature for an hour and later dried in an oven at 90˚c for 30 minutes. Membrane dimensions, before and after shrinkage were measured by using images taken on EVOS XL microscope (Thermo Fisher Scientific, USA) and analyzed using ImageJ.

Shrinking of embedded microchannels

Custom G-code was used to print 47mm x 47mm isomalt mesh with repeating square units (grids). PDMS+ST mixture was prepared with 70% wt ST and cast on a glass petri dish. This was partially cured at 90˚C for 6minutes and cooled to room temperature. Isomalt mesh was placed over this semi-cured base layer and another layer of PDMS+ST was cast over the isomalt mesh. This was placed in an oven at 40˚C for 48 hours to cure without deforming the isomalt structure inside. 2cm x 2cm samples were punched out from this configuration and immersed in water to dissolve away the isomalt. These were subjected to 48 hours solvent treatment in IPA and later dried in an oven at 90˚C for 30 minutes. SEM images (TESCAN VEGA) were taken for cross-sections before and after solvent treatment.

Fabrication of oxygenator devices

The g-code for 47mm x 47mm was modified to include a pair of inlet-outlet configurations at diagonal ends (Figure 2) and printed at 300kPa – 200mm/min. A layer of PDMS+ST (70% wt ST) was initially spincoated at 1500rpm for 5 seconds and a PTFE mesh layer (1 µm pore size, 83% porosity, and ~35 µm thick) was embedded for device integrity. PDMS+ST was spincoated over the PTFE layer at 500rpm for 5 seconds, cured over a hotplate at 90˚C for 3 minutes and cooled to room temperature. The isomalt structure was placed over this layer and another layer of PDMS+ST was spincoated at 500rpm for 3 seconds. The samples were placed in an oven at 40˚C for 48 hours to cure without deforming the isomalt structure inside. The devices were immersed in water to dissolve the isomalt and later solvent treated in IPA for 48 hours to shrink the device. Microscope images were taken for top-view and cross-sections before and after solvent treatment.

RESULTS AND DISCUSSION

Impact of printing parameters

Three different extrusion pressure levels (200 kPa, 300 kPa and 400 kPa) were used to extrude isomalt at various speeds in 50 mm/min to 700 mm/min range (Figure 3). Width increased as the extrusion pressure was increased and decreased as the printing speed was increased. For a constant layer height (~200±23 µm), it was observed that at low pressures or at high printing speeds, the filament deposition was not continuous and droplet deposition occurs. This transition defines the resolution limit of the deposition possible, and the thinnest filament deposited was 127µm wide, at 200kPa and 550mm/min.

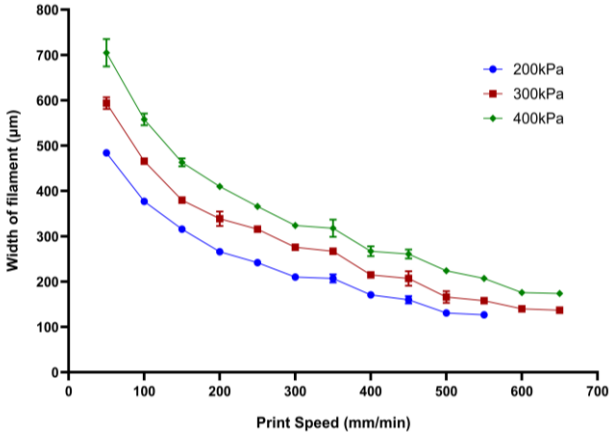

Figure 3: Impact of printing parameters on filament width

Shrinking characteristics of thin membranes

PDMS+ST membranes, <500µm thick with 70% wt ST, were exposed to IPA for three days. Initially, rapid weight loss occurred, followed by slower reduction and stabilization at the end of 48 hours (Figure 4a). The dominant migration of the thinner components towards the solvent side was primarily due to the higher concentration gradient, with the migration rate slowing as the gradient diminished. The plot of achievable weight loss using different solvents is presented in Figure 4b. IPA and acetone treated samples showed the maximum capability to shrink the membranes, while water showed negligible capability to shrink. This disparity is attributed to these solvents' greater ability to induce swelling in the PDMS compared to the other solvents utilized in the study. Although the amount of thinner was at 70% wt ST, the observed weight loss percentage was slightly higher, which indicates the extraction of uncured PDMS chains from the matrix, along with the thinner. Figure 4c emphasizes how the shrinking behavior is dependent on the concentration of ST in the sample. Samples with more ST shrinks more and concentration of the thinner impacts the cross-linking process, with excessively high concentrations resulting in unsuccessful curing of the samples.

Shrinking of embedded microchannels in thick membranes

Isomalt meshes were produced based on the previously established parameters, with channel spacing of 600µm, followed by the casting of PDMS+ST (70% weight ST) over the sacrificial template. The samples underwent curing at 40˚C for 48 hours, after which the isomalt was dissolved. The resulting channels had a width of ~560µm and height of ~140µm, and an inter-channel spacing of ~610µm. After thinner extraction in IPA, final shrunken samples, resulted in dimensions of ~340µm wide and ~170µm tall channels, and the inter-channel spacing reduced to ~398µm (Figure 5).

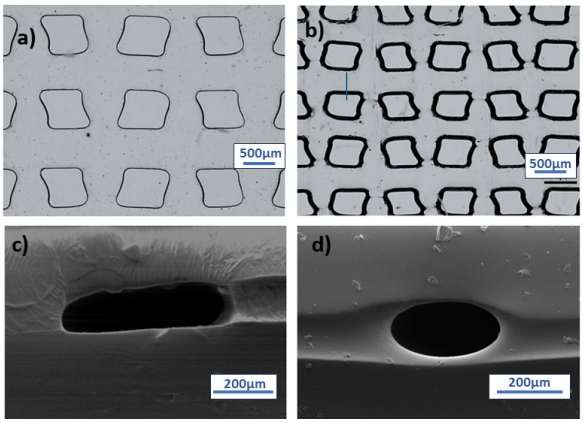

Figure 5: Microscopic images showing shrinkage in embedded channels, topview (a) before (b) after shrinkage, and cross-sectional view (c) before and (d) after shrinkage.

Fabrication of oxygenator devices

Devices were made using meshes defined by filaments spaced 800µm apart in the g-code. The dimensions of the channel before and after shrinkage are illustrated in Figure 6, followed by their measurements in Table 1. From the shrinking, it was observed that there was only <10% reduction in both the channel width and spacing in Y while in X, the width reduced by ~19±5% and spacing reduced by ~36±5%. It can be hypothesized that the non-uniform shrinkage across directions may be induced by the constraints introduced in the silicone matrix, including the base PTFE

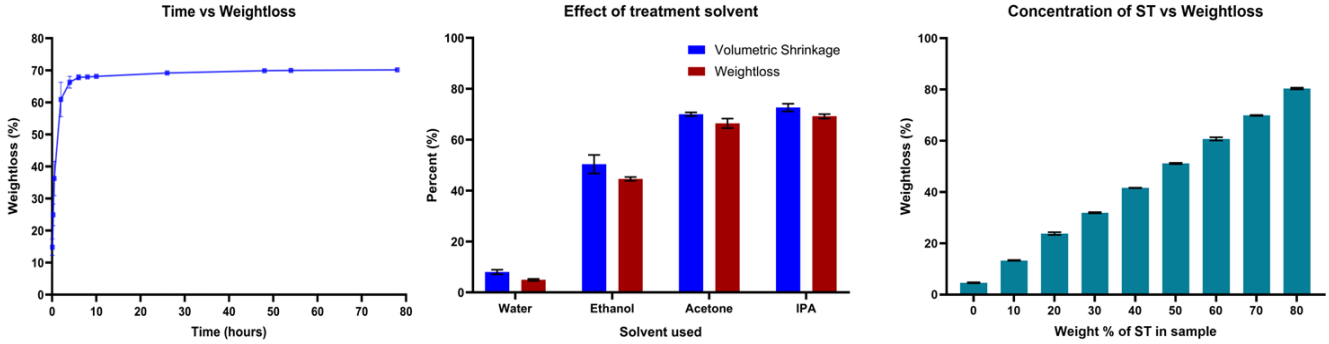

Figure 4: Shrinkage process characterization of thin membranes (a) Identifying solvent treatment time window by monitoring weight loss percent (b) Effect of various treatment solvents on dimensional shrinkage (c) Effect of silicone thinner concentration in achievable shrinkage, using isopropanol treatment.

membrane and the silicone tubings at inlet/outlet. This is furthermore evident from the resulting membrane topology where the PTFE introduced wrinkles on the membrane (Figure 7). The cross-sections of the shrunken devices with thin membranes were difficult to image, owing to (i) warping of the entire device (ii) wrinkling of membrane and (iii) top-bottom membranes collapsing over the channel section. Proper handling and framing of the shrunken device are necessary in studying how the shrinkage happens in cross-section and for further *in-vitro* tests.

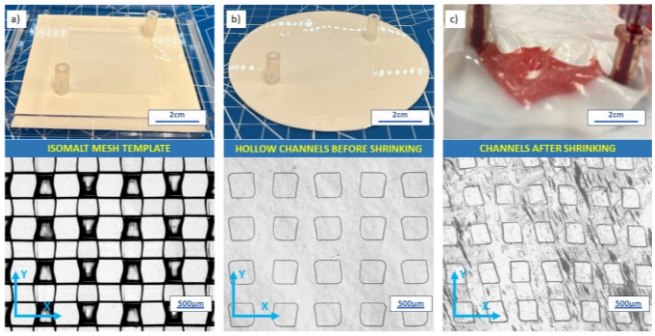

Figure 6: (a) Isomalt mesh printed and its microscopic image (b) Device fabricated and the microscopic image of channels, and (c) the device after shrinkage, filled with blood before and its shrunk dimensions. The texture visible over the shrunk membrane surface is the wrinkles from PTFE base membrane.

	Before	After
Channel width (X)	319±5µm	257±16µm
Channel width (Y)	361±5µm	334±8µm
Spacing (X)	472±13µm	301±18µm
Spacing (Y)	407±8µm	368±9µm

Table 1: Device channel dimensions before and after shrinking.

Figure 7: The shrinking of PDMS+ST attached to a PTFE base membrane introduces wrinkles over the membrane as illustrated by the microscopic top-view of the membrane (with embedded channels).

CONCLUSIONS

Sacrificial 3d-printing has never been used to fabricate microfluidic oxygenator devices owing to the resolution limits and the unavailability of a suitable protocol. We present a hybrid approach where it can be introduced to the oxygenator fabrication avenue. This serves as a notable proof-of-principle for the fabrication and offers a new utility for oxygenator manufacturing. The composite membrane with PTFE offered structural integrity, but altered the way the devices shrink. It would be ideal to have the device shrink without the PTFE mesh, attach it later for perfusion and *in-vitro* testing. Future efforts will be to optimize the fabrication protocol to achieve thin membrane devices and subsequently subject them to *in-vitro* gas exchange testing using blood.

ACKNOWLEDGEMENTS

We acknowledge financial support from the Canadian Institutes for Health Research (CIHR). PRS acknowledges support from McMaster University for the Distinguished Engineering Professor award.

REFERENCES

[1] Dabaghi M, Rochow N, Saraei N, Mahendran RK, Fusch G, Chan AKC, et al. Miniaturization of Artificial Lungs toward Portability. Adv Mater Technol. 2020 Jul 1;5(7):2000136

[2] Potkay JA. The promise of microfluidic artificial lungs. Lab Chip. 2014 Sep 30;14(21):4122–38

[3] Kniazeva T, Epshteyn AA, Hsiao JC, Kim ES, Kolachalama VB, Charest JL, et al. Performance and scaling effects in a multilayer microfluidic extracorporeal lung oxygenation device. Lab Chip. 2012 Apr 3;12(9):1686–95

[4] Gimbel AA, Hsiao JC, Kim ES, Lewis DJ, Risoleo TF, Urban JN, et al. A high gas transfer efficiency microfluidic oxygenator for extracorporeal respiratory assist applications in critical care medicine. Artif Organs. 2021 Aug 1;45(8):E247–64.

[5] Dabaghi M, Rochow N, Saraei N, Fusch G, Monkman S, Da K, et al. A Pumpless Microfluidic Neonatal Lung Assist Device for Support of Preterm Neonates in Respiratory Distress. Advanced Science. 2020 Nov 1;7(21).

[6] Thompson AJ, Ma LJ, Major T, Jeakle M, Lautner-Csorba O, Goudie MJ, et al. Assessing and improving the biocompatibility of microfluidic artificial lungs. Acta Biomater. 2020 Aug 1;112:190.

[7] Santos JA, Gimbel AA, Peppas A, et al. Design and construction of three-dimensional physiologically-based vascular branching networks for respiratory assist devices. Lab Chip. 2021 Nov 25;21(23):4637–51.

[8] Chen C, Hirdes D, Folch A. Gray-scale photolithography using microfluidic photomasks. Proc Natl Acad Sci U S A. 2003 Feb 18;100(4):1499–504.

[9] Koh KS, Chin J, Chia J, Chiang CL. Quantitative Studies on PDMS-PDMS Interface Bonding with Piranha Solution and its Swelling Effect. Micromachines 2012, Vol 3, Pages 427-441. 2012 May 4;3(2):427–41.

[10] Gelber MK, Bhargava R. Monolithic multilayer microfluidics via sacrificial molding of 3D-printed isomalt. Lab Chip. 2015 Mar 17;15(7):1736–41.

[11] Hamidi A, Tadesse Y. 3D printing of very soft elastomer and sacrificial carbohydrate glass/elastomer structures for robotic applications. Mater Des. 2020 Feb 1;187:108324.

[12] Nadernezhad A, Ryma M, Genç H, Cicha I, et al. Melt Electrowriting of Isomalt for High-Resolution Templating of Embedded Microchannels. Adv Mater Technol. 2021 Aug 1;6(8).

[13] Hassan I, Selvaganapathy PR. Microfluidic Printheads for Highly Switchable Multimaterial 3D Printing of Soft Materials. Adv Mater Technol. 2022 Sep 1;7(9).

CONTACT

*P. Ravi Selvaganapathy, selvaga@mcmaster.ca